Perspective

Nanocatalysts in electrosynthesis

Honghong Lin,[1] Kecheng Wei,[1] Zhouyang Yin,[1] and Shouheng Sun[1,*]

SUMMARY

Electrosynthesis is to use electricity to drive chemical reactions for chemical synthesis and is potentially a green approach to fuel and energy sustainability. Nanostructured catalysts play an important role in promoting electrochemical reactions under green chemistry conditions. This perspective first provides a brief tutorial on electrosynthesis and the roles the nanocatalysts play in the synthesis. It then outlines the common strategies used to develop nanocatalysts for hydrogen evolution reaction, CO_2 reduction reaction, and biomass upgrading. The perspective further summarizes the current methodologies that have been developed for scaling-up synthesis of nanocatalysts, which will be essential for the electrosynthesis to become a viable industry approach.

INTRODUCTION

Chemical manufacturing requires to burn a significant amount of fossil fuels for its energy needs, which account for about a quarter of the world's energy demand (Blanco and Modestino, 2019). This contributes in large part to the fast depletion of fuel resources from nature's reserves and the unprecedented accumulation of CO_2 in our living environment. Using electricity to drive chemical reactions can, in principle, mitigate fuel depletion and CO_2 emission problems. Currently, only a small fraction of the manufacturing processes are electrochemically based due to the lack of cost-effective carbon-neutral ways of generating electricity (Botte, 2014; Kevin et al., 2019). Over the past decades, however, the much increased capacity and decreased cost of renewable electricity (Figure 1A) ("Solar PV Cumulative Capacity, 1976 to 2016"; "Solar PV Module Prices, 1976 to 2016") make it appealing to incorporate electricity into the chemical reaction processes. More and more research data have suggested that renewable electricity is key to reducing fossil fuel consumption and CO_2 emission, as well as to developing the much needed green chemistry solutions to chemical manufacturing processes.

ELECTROSYNTHESIS

Electrosynthesis is a chemical synthetic process powered by electricity, in which chemical reactions are initiated and controlled by electrochemical reduction or oxidation potentials. A basic electrochemical cell used for electrosynthesis is shown in Figure 1B. In an electrosynthetic process, the renewable electricity supplies the power to initiate oxidation (on anode) and reduction (on cathode) reactions with two electrode compartments being separated by an ion-conducting polymer membrane. Successful examples of electrosynthesis in the industry have been demonstrated in the chlor-alkali process to make Cl_2 and NaOH, Hall-Héroult process to prepare elemental Al, and the Monsanto process to synthesize adiponitrile, a key intermediate for nylon production (Botte, 2014). Compared with conventional thermochemical reactions, these electrochemical ones avoid the stoichiometric uses of chemical oxidants or reductants and can proceed under ambient reaction conditions, which makes it convenient to monitor reactions in situ (Li and Sun, 2018). With these benefits and promises, electrosynthesis has attracted much attention recently not only in small molecule reactions, such as water splitting for H_2 generation and CO_2 reduction for hydrocarbon formation, but also in large molecule conversions, such as biomass upgrading (Orella et al., 2018).

CATALYST IN ELECTROSYNTHESIS

Catalysts have played an important role in chemical manufacturing—more than 85% of existing processes rely on catalysts (Schaidle et al., 2017). Great economic values the catalysts have created continue to drive the catalyst research and development to lower reaction energy barriers and improve reaction kinetics (Figure 2A) under green chemistry reaction conditions. In an electrochemical process, the working potential (E_{WE}) required to promote a reaction is decided by not only the standard potential (E_0) but also the resistance overpotential (η_R), concentration overpotential (η_C), and activation overpotential (η_A) (Equation 1).

[1]Department of Chemistry, Brown University, Providence, RI 02912, USA
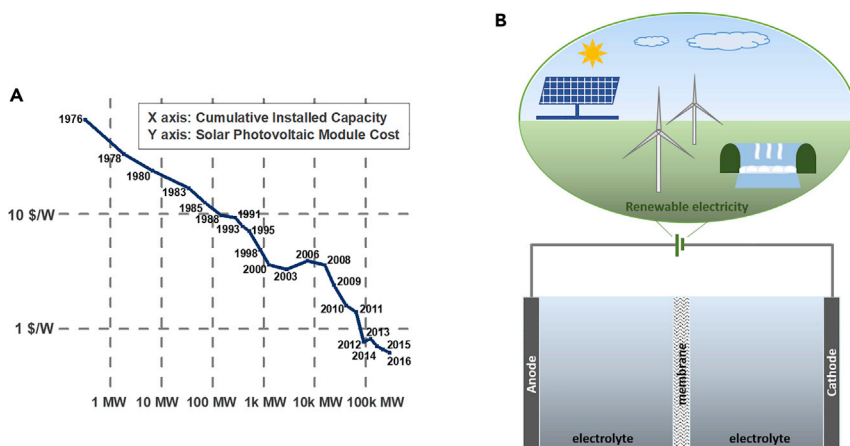
*Correspondence: ssun@brown.edu

Figure 1. The price trend of renewable electricity and the schematic of renewable energy powered electrosynthesis
(A) The solar photovoltaic module prices (measured in US dollar per watt, $/W) versus cumulative capacity (measured in megawatts, MW) from 1976 to 2016.
(B) A basic setup for electrosynthesis, consisting of a power supply, an anode, a cathode, and a polymer membrane to separate two electrodes in the reaction electrolyte. The power is generated from any of the renewable solar, wind, or hydropower sources.

Resistance overpotential is tied to the cell design, the concentration overpotential is more often observed at the high current region, and the activation overpotential is largely determined by the catalyst (Barbir, 2013). Therefore, designing a stable catalyst that can catalyze the electrochemical reaction with high activity and selectivity is the first critical step toward the successful development of an efficient and cost-effective electrosynthesis process.

$$E_{WE} = E_0 + \eta_R + \eta_C + \eta_A \qquad \text{(Equation 1)}$$

Both homogeneous and heterogeneous catalysts are studied for electrosynthesis (Zhang et al., 2020b). Homogeneous electrocatalysts have well-defined coordination chemistry, and their catalytically active sites can be designed around the coordination centers (Figure 2B(a)). They are especially suitable for reaction kinetics studies to achieve high reaction selectivity. However, there are two challenging issues in applying these homogeneous catalysts for electrosynthesis: their non-recyclability and their entangled mixing with reaction products, which make them costly and energy inefficient to use. Therefore, homogeneous catalysts are commonly applied in lab scales to evaluate electrocatalytic reaction mechanisms (Rønne et al., 2020), which are important for discovering new electrosynthesis reactions (Siu et al., 2020).

As a comparison, heterogeneous electrocatalysts are present in different phases from reactants and are structurally more stable than the homogeneous ones (Figure 2B(b)). They can be separated from reaction products easily and be reused for the next round of reactions. Heterogeneous catalysts are often made of solid nanoparticles (NPs) supported on conductive supports. Recent advances in NP synthesis enable the preparations of NPs with controlled sizes, shapes, compositions, and crystal structures. These allow more rational tuning of catalysis to select energy-efficient reaction pathways, leading to the optimized reaction outcomes (Ding et al., 2019; Muzzio et al., 2019). It is worth to mention that heteroatom-doped carbon materials with atomically active sites have become an attractive class of heterogeneous catalysts as they combine the merits of common heterogeneous catalysts' recyclability and homogeneous catalysts' high atom utilization (Lu et al., 2020a). However, these "atomic" catalysts do not yet have the desired distribution and mass controls of the heteroatoms across the carbon networks, which are important for them to achieve industry-relevant catalytic activities (Lei et al., 2020b).

EXAMPLES OF ELECTRO-CATALYZED REACTIONS

Hydrogen evolution reaction

Hydrogen (H_2) is both an attractive fuel for clean energy production and an important reagent for hydrogenation reactions in the chemical industry. Currently, H_2 is mostly produced from steam reforming of fossil
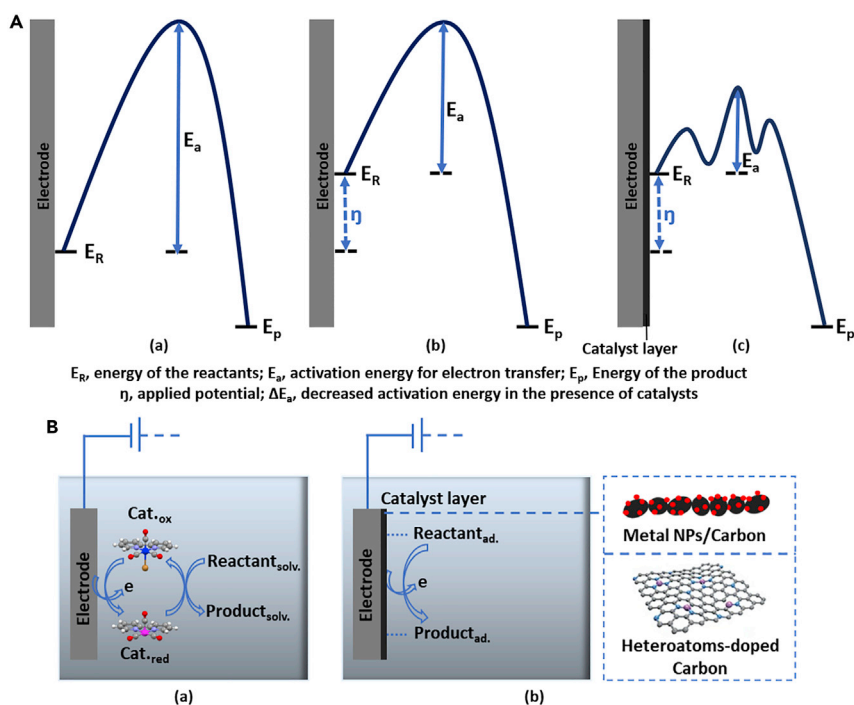
Figure 2. Schematic activation energy change of a thermodynamically favored electrochemical reaction
(A) (a) Energy diagram of a reaction on a bare electrode, (b) energy diagram of a reaction on an electrified electrode, (c) energy diagram on a catalyst-modified electrified electrode.
(B) Different catalytic mechanism of (a) a homogeneous catalyst and (b) a heterogeneous catalyst in electrocatalysis.

resources. An alternative, and yet more attractive, approach of producing H_2 is water splitting by renewable electricity. In catalyzing this water splitting reaction, noble-metal-based catalysts (mostly Pt, Pd, Ru) generally outperform non-noble-metal-based ones (Mo, Fe, Co, Ni, W, V, Cu, etc.) in terms of activity and stability—up to 80-90% of energy efficiencies can be achieved with noble-metal-based catalysts in proton exchange membrane electrolyzers (Millet et al., 2010). Recent research focuses are on (1) increasing noble metal utilization by decreasing physical sizes of these noble metal catalysts to cluster at an atomic level or diluting the noble metal distributions by alloying them with other elements and (2) enhancing the activity of non-noble-metal-based catalysts by increasing active sites, introducing defects, doping heteroatoms, or tuning phases (Zhu et al., 2020). At this stage, the activity gap between the non-noble-metal-based catalysts and noble-metal-based (especially Pt based) catalysts is still significant, but from the cost perspective, the non-noble-metal catalysts are still attractive for practical applications if they can be made stable in water splitting reaction media.

Encapsulating non-noble-metal-based catalysts with carbon shells is a common strategy to improve catalyst stability. A carbon shell can be deposited on NPs via chemical vapor deposition (Shen et al., 2018), high-temperature co-annealing with a proper carbon source (Dong et al., 2017; Ma et al., 2017; Yang et al., 2018), or pyrolysis of Metal-organic frameworks (MOFs) (Wang et al., 2018a), as illustrated in Figure 3A. A good example of this carbon coating effect on catalysis enhancement was shown in FeP-catalyzed hydrogen evolution reaction (HER), as summarized in Figure 3B (Dong et al., 2017). In this study, FeP was found to be active for the HER and the carbon coating did not affect its catalysis activity, rather, it effectively stabilized the FeP catalyst under the HER condition (Figure 3C) (Dong et al., 2017). However, it is not clear if this carbon coating strategy can be generalized to stabilize non-noble metal catalysts for HER. More studies on coating thickness, porosity, and uniformity for NP stabilization are needed.

An alternative strategy to stabilize a non-noble metal is via its alloying with a noble metal, such as Pt or Pd, to form a chemically ordered intermetallic structure. The formation of the intermetallic $L1_0$-MPt (M= Fe or Co) from its solid solution counterpart is shown in Figure 3D. In this $L1_0$-MPt structure, M and Pt stack alternately along the crystallographic c-direction due to the strong M (3d)-Pt (5d) coupling, and M is tightly
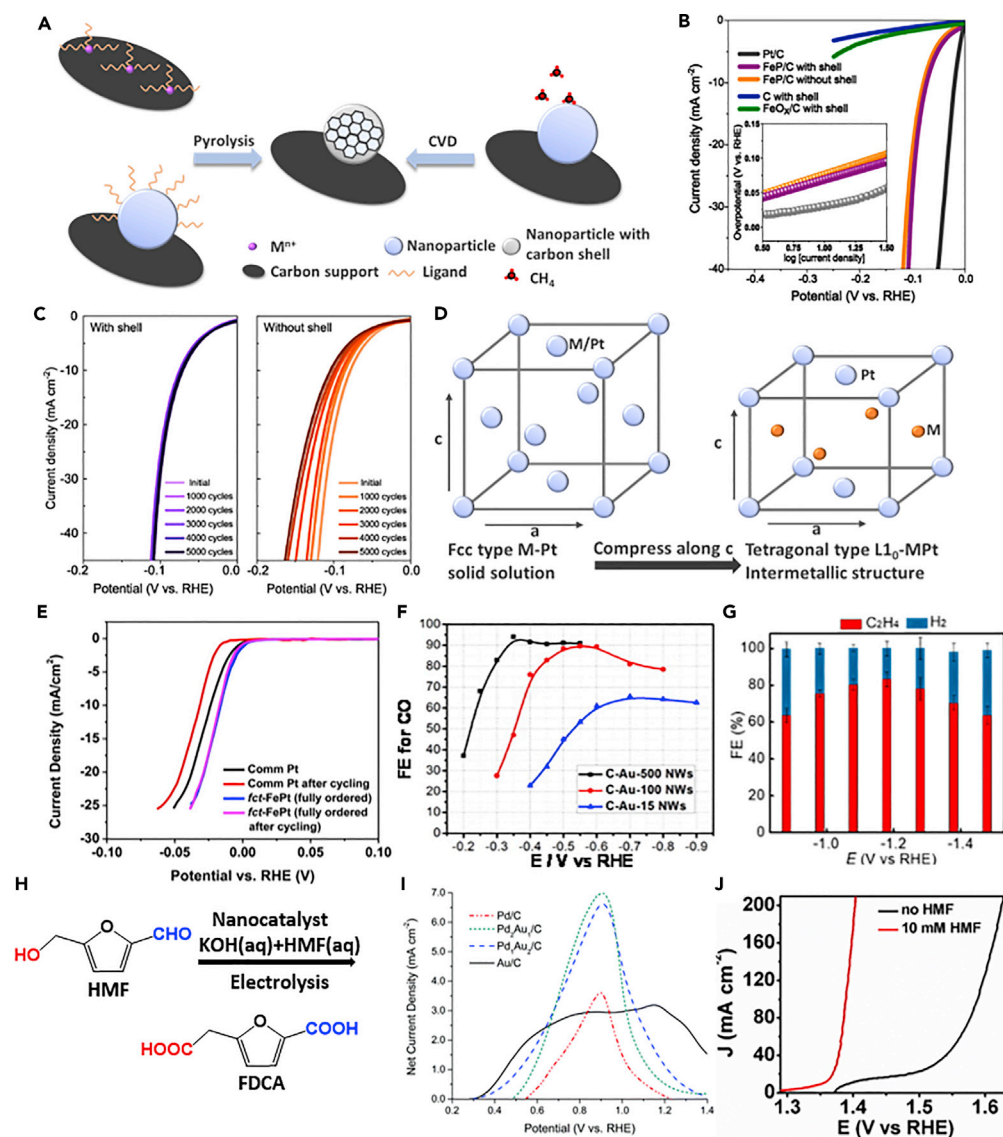
Figure 3. Nanocatalysts and their catalysis applied in electrosynthesis

(A) Schematic of coating an NP catalyst with a carbon shell.

(B) FeP-catalyzed HER with FeP covered without and with the carbon shell, and their catalysis comparison with commercial Pt, carbon shell, and iron oxide coated with the carbon shell. Adapted with permission from (Dong et al., 2017). Copyright 2017, American Chemical Society.

(C) HER stability test of the FeP catalyst with (left) and without (right) a carbon shell. Adapted with permission from (Dong et al., 2017). Copyright 2017, American Chemical Society.

(D) Structure conversion from fcc-type solid solution of M-Pt/Pd alloys to tetragonal $L1_0$-MPt/Pd intermetallic alloys, M= Fe or Co.

(E) HER polarization curves before and after 10 k cycles of commercial Pt and $L1_0$-FePt (fct-FePt). Adapted with permission from (Li et al., 2015). Copyright 2015, American Chemical Society.

(F) Potential-dependent FE of CO_2 to CO on ultrathin Au NW catalysts with different lengths (500 nm, 100 nm, 15 nm). Adapted with permission from (Zhu et al., 2014). Copyright 2014, American Chemical Society.

(G) Potential-dependent FE of CO_2RR products on nanodefective Cu nanosheet catalysts. Adapted with permission from (Zhang et al., 2020a). Copyright 2020, American Chemical Society.

(H) Electrooxidation of HMF to FDCA in the presence of a nanocatalyst.

(I) Anodic scan of half-cell cyclic voltammetry in the presence of an NP catalyst in 0.1 M KOH with 0.02 M HMF at 25 °C. Adapted with permission from (Chadderdon et al., 2014). Copyright 2014, Royal Society of Chemistry.

(J) Anodic scan of half-cell cyclic voltammetry on Ni_3S_2/Ni foam catalysts in 1.0 M KOH with and without 10 mM HMF at 25 °C. Adapted with permission from (You et al., 2016). Copyright 2016, American Chemical Society.

sandwiched by the Pt layers and efficiently stabilized. The HER performance of the $L1_0$-FePt was much enhanced than the commercial Pt catalyst due to the Fe-alloy effect and Fe stabilization against acid etching (Figure 3E) (Li et al., 2015). In general, the formation of an intermetallic structure requires careful controls of the alloy compositions and annealing conditions (Li and Sun, 2019). The intermetallic alloys of non-noble metals are also studied, but the structure cannot stabilize metals against dissolution under the electrocatalytic reaction conditions (Menezes et al., 2018; Sun et al., 2018).

More strategies adopted to increase the HER activities of the metal NP catalysts were discussed in more details in a recent review (Zhu et al., 2020). There have been many reports demonstrating that non-noble metal NPs can show HER activities comparable to noble metal ones. These non-noble metal NPs need to be scrutinized more carefully before their catalysis potentials can be fully realized for HER in practical proton exchange membrane electrolyzers.

Carbon dioxide reduction reaction

Reducing carbon dioxide (CO_2) into hydrocarbon products by renewable electricity under ambient conditions is a direct response to fast depletion of fossil fuels and uncontrolled CO_2 accumulation in our surroundings. Critical issues about this CO_2 reduction reaction (CO_2RR) are in (1) increasing the reduction selectivity toward hydrocarbon products over side HER that produces H_2, (2) increasing the selectivity toward a specific hydrocarbon product rather than a mixture of products, and (3) decreasing the reaction overpotential to make the reaction more energy efficient (Xie et al., 2020).

So far, the reduction Faradaic efficiency (FE) toward carbon monoxide (CO) or formate ($HCOO^-$) can reach more than 90% (Wen et al., 2020; Zhou et al., 2019; Zhu et al., 2014). An example of tuning electrocatalytic reduction of CO_2 to CO is shown in Figure 3F, where ultrathin (2 nm wide) Au nanowires were studied as the catalyst to show nanowire length-dependent conversion efficiency (Zhu et al., 2014). The longer nanowires (500 nm) show much enhanced CO formation efficiency (94%) at -0.35 V (vs RHE) due to the maximal exposure of the active Au edge sites along the nanowire for CO_2 activation and reduction.

However, achieving high FE toward hydrocarbon products is still challenging, and Cu is an essential catalyst component for promoting C-C bond formation (Hori et al., 2003; Popović et al., 2020). Current strategies applied to increase the FE of the hydrocarbon products on Cu-based catalysts include the following: (1) constructing grain boundaries and defects (Lei et al., 2020a; Wang et al., 2018b; Zhang et al., 2020a), (2) controlling exposed facets of NPs that favored C_{2+} product over C_1 product (Hori et al., 2003; Loiudice et al., 2016; Yin et al., 2019), (3) improving local structure to facilitate *CO binding and *CO-*CO coupling (Wang et al., 2020), and (4) modifying the catalyst surface with molecular additives to control pH gradient at the reaction interface to enhance CO_2 adsorption and activation (Han et al., 2017; Nam et al., 2020; Ovalle and Waegele, 2019; Thevenon et al., 2019). To date, high-performance catalysts can convert CO_2 to ethylene and other C_{2+} products with FE higher than 60% (Thevenon et al., 2019; Wang et al., 2020; Yin et al., 2019). The highest ethylene formation FE 83.2% is obtained when a defective Cu nanosheet catalyst is present to concentrate CO and OH^- in the CO_2 reduction process (Figure 3G) (Zhang et al., 2020a).

In general, lowering the activation energy of the intermediates on the catalyst surface is critical to generate C_{2+} product, but to find the exact catalysis tuning knob requires a more rational design of the catalyst surface and a deeper understanding of reaction mechanisms at atomic and molecular levels. Catalysts capable of achieving high FE to C_1 products have been reported recently, and it is expected that these catalysts will be investigated thoroughly in membrane electrode assembly systems to demonstrate their scaling-up potentials for electrochemical conversion of CO_2 (Chen et al., 2020; Dinh et al., 2019; Fan et al., 2020).

Biomass upgrading

Electrocatalysis has also been applied to convert biomass products to high-value platform chemicals. 5-hydroxymethylfurfural (5-HMF) is a representative precursor chemical obtained from biomass hydrolysis (Kwon et al., 2016). Electro-oxidation of 5-HMF can proceed without using any hazardous oxidant or pressurized O_2 to form 2,5-furandicarboxylic acid (FDCA) (Figure 3H) that is suitable for green polymer production (Zhao et al., 2018). The reaction could be catalyzed by noble-metal Pt, Pd, Au, and Pd-Au NPs (Chadderdon et al., 2014; Rao Vuyyuru and Strasser, 2012; Zhao et al., 2018), especially $PdAu_2$ NPs with which FDCA was obtained at a 83% yield with 100% conversion at 0.9 V (vs. RHE) in the aqueous solution of
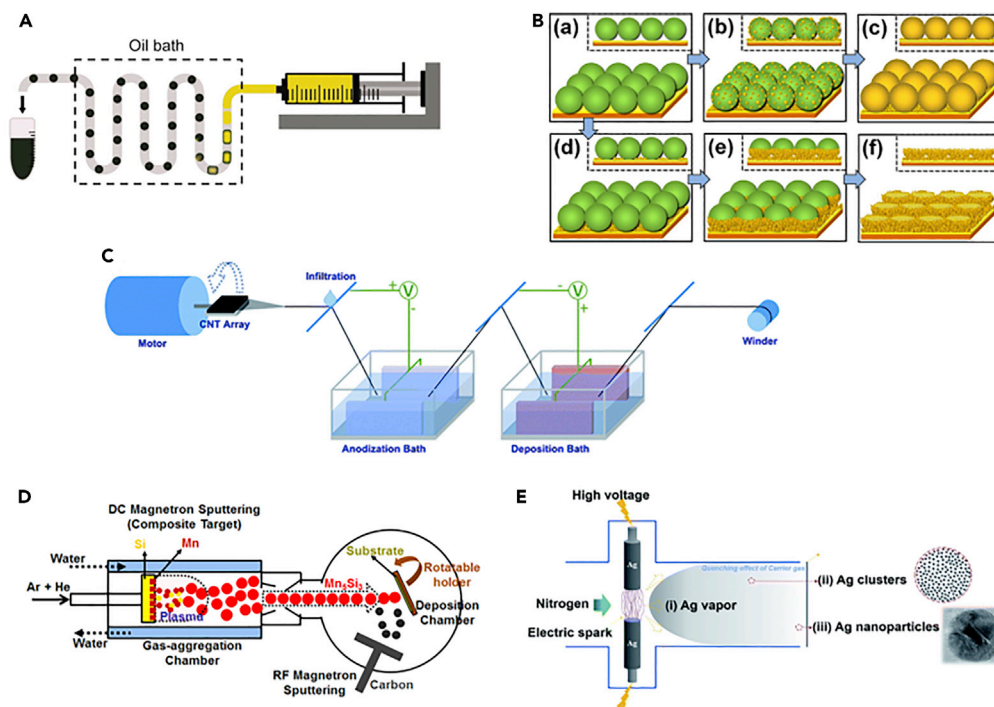
Figure 4. Schematic of some representative reaction systems for scaling-up syntheses of NPs

(A) A continuous flow cell reactor with droplets inside as separated reactors to make monodisperse NPs. Adapted with permission from (Niu et al., 2016). Copyright 2016, American Chemical Society.

(B) A template-based electrodeposition method to prepare hierarchically micro/nanostructured NP arrays (yellow substrate—Au film on indium oxide coated glass; green spheres—polystyrene particles). Adapted with permission from (Wang et al., 2019). Copyright 2019, Elsevier.

(C) A continuous electrodeposition system used to fabricate carbon nanotube-Cu fibers. Adapted with permission from (Xu et al., 2011). Copyright 2011, Royal Society of Chemistry.

(D) A cluster deposition system for solventless NP synthesis. Adapted with permission from (Das et al., 2016). Copyright 2016, American Chemical Society.

(E) A spark ablation system for solventless NP synthesis. Adapted with permission from (Lu et al., 2020b). Copyright 2020, Royal Society of Chemistry.

0.02 M 5-HMF + 0.1 M KOH (Figure 3I). Non-noble-metal-based Ni- (Taitt et al., 2019; You et al., 2016; Zhao et al., 2018), Fe- (Taitt et al., 2019; Zhao et al., 2018), and co-catalysts (Huang et al., 2020; Taitt et al., 2019; Zhao et al., 2018) were also active for catalyzing this oxidation reaction at more positive potentials (>1.4 V vs. RHE) (Figure 3J), which is much higher than the standard potential (0.68 V vs. RHE) (Kwon et al., 2016). Future studies should focus on lowering the oxidation potential to improve energy efficiency and on improving the catalyst stability in the reaction media where an alkaline condition is required to maintain good solubility of FDCA.

SCALING-UP SYNTHESIS OF ELECTROCATALYSTS

A practical electrocatalyst must be produced in a mass scale. The criteria to evaluate the scaling potentials of a good nanocatalyst synthesis lie in NP quality control, synthetic yield, synthesis cost, and environmental impact. Scaling up the synthesis from the lab scale is always challenging as the heat and mass transport issues are often difficult to overcome in mass-scale reactions to control NP nucleation and growth. From the synthesis point of view, yield and product quality are currently the main concerns.

Monodisperse metal oxide NPs were first prepared at 10's gram level from single batch thermal reactions of metal chlorides and sodium oleate (Park et al., 2004). This method was extended to synthesize other metal, metal oxide, and even metal phosphide NPs (Dong et al., 2017). To improve the heat and mass transfer in large volume reaction systems, a continuous flow cell reactor design (Figure 4A) was introduced (Niu et al.,

2016; Zhang et al., 2014). This flow cell allows careful control of the flow rate of the reaction solution and, in the meantime, realizes uniform heat and mass transfer. With this continuous flow cell reactor, Au, Pd, Pd-M (M = Pt, Au, and Ag), and octahedral NiPt NPs were synthesized at the mass rate of 1-10 gram per hour (LaGrow et al., 2017; Niu et al., 2016; Zhang et al., 2014). In addition, by controlling the flow rate or adding tungsten carbonyls (which will generate carbon monoxide when decomposing), the reaction solution flow could be interrupted to turn the continuous flow into consecutive droplets within which further promoted the heat and mass transfer and improved the NP quality. This method has been used to prepare a series of metal and metal alloy NPs (LaGrow et al., 2017).

One obvious issue with either the batch reactor or the continuous flow reactor is that each synthesis requires a large volume of solvent in both reaction and product purification processes, which inevitably generate a considerable amount of waste in a large-scale synthesis. Conventional electrodeposition in aqueous solution was recently re-introduced as an attractive alternative to large-scale synthesis. In this approach, electrochemical reduction or oxidation is simply controlled by the electric potential in water without the need of any chemical reductant or oxidant, providing an appealing process to green chemistry synthesis of NPs. Although the quality of the NPs produced from the electrodeposition method is generally lower than that from the solution-phase reactions, well-defined nanostructures can be obtained by using proper templates (Figure 4B). For example, Au substrate or polystyrene spheres were used to control the nucleation of Au to form quasi-spheres and further grow into different hierarchical nanostructures (Figure 4B(c, e, f)) (Wang et al., 2019). For the large-scale synthesis, a continuous electrodeposition method could be adopted, as demonstrated in the deposition of nanostructured Cu onto the rolling carbon nanotube fiber in the deposition bath and collected via a winder (Figure 4C) (Xu et al., 2011). In this study, the deposition bath is adjusted to deposit a different metal component to form core/shell structure and to clean NP surface. The catalyst product can be peeled off from the rolling band, realizing continuous product output.

Compared to any of the above scaling-up synthetic approaches, a physical deposition process without using any solvent and surfactant is certainly more attractive for green chemistry synthesis of electrocatalysts. And the surfactant-free condition also provides a clean NP surface for electrocatalysis. A representative example is the cluster deposition, as shown in Figure 4D, in which bulk solid precursors are first sputtered with a high energy Ar/He beam, and the sputtered atoms are then condensed, extracted, and deposited onto the substrates (Das et al., 2016). The sizes and structures of NPs can be controlled by the chamber pressure—higher pressure leads to more atom collisions and larger particle size—and by in-flight annealing (Akdogan et al., 2011). Transition metal NPs, including some very air-sensitive rare-earth metal alloy NPs, have been synthesized by this method (Abbas et al., 2019; Balasubramanian et al., 2016; Das et al., 2016). Spark ablation is another method developed for NP synthesis in the solvent/surfactant-free environment. In this method, the metal vapor is generated by an electrode and quenched by an inert gas flow to form NPs (Figure 4E) (Lu et al., 2020b). The sizes of the NPs are controlled by potentials, currents, and carrier gas flow rates. As a facile and green method, spark ablation has been commercialized (VSParticle) for large-scale synthesis of metal and metal oxide NPs with a touch of a button (Lu et al., 2020b; Tabrizi et al., 2009).

Each of the synthetic method mentioned above has its pros and cons, and more research studies are still needed to expand the advantages and to minimize the undesired negative impacts of each method. For example, the continuous flow cell reactor may be investigated to synthesize mono-/multi-metallic NPs with diverse nanostructures (Santana and Skrabalak, 2020; Santana et al., 2017) but with solvents/surfactants being recycled for the next round of synthesis. In the electrodeposition method, an in-line electrocatalytic screening technique may be incorporated to monitor the NP formation in situ so that the NP growth can be controlled in a more rational way and no post-synthesis characterizations are needed. The versatility of NP growth during the cluster deposition and spark ablation may be further improved by introducing proper templates.

CONCLUSION

The development of electrosynthesis is an important step toward a greener and more sustainable industry, and finding efficient nanocatalysts is essential to make the synthesis practical for industrial applications. Past studies have demonstrated the great potentials of nanocatalysts in promoting electrosynthesis under green chemistry conditions, but major challenges still exist. For example, using HER to produce H_2 often

requires noble metal catalysts; common transition metal nanocatalysts are much less active and are too unstable to be practical. Electrochemical reduction of CO_2 to hydrocarbons occurs only on the Cu-containing catalyst surfaces, and yet the Cu catalysts tend to restructure under the negative CO_2RR conditions. Electrochemical biomass upgrading also requires the presence of noble metal nanocatalysts as non-noble metal ones are neither as active nor as stable. A full understanding of these electrocatalysis reactions requires the mass production of nanocatalysts to provide continuous support of reliable nanocatalysts for studying these reactions. Various synthetic methods, including the batch reactor method, continuous flow method, electrodeposition method, and even solventless physical deposition method, have been explored to scale-up the syntheses, but each of these methods has its own pros and cons in reaching the goals for industrial-scale green chemistry synthesis. More studies are still needed to achieve the desired nanostructure and catalysis controls. With the non-stopping supply of reliable nanocatalysts, more electrochemical reactions, including electrocatalytic tandem reactions, can be studied and applied to simplify synthetic procedures, making the electrosynthesis a true green chemistry approach to high value chemicals and fuels for sustainable chemistry and energy applications.

AUTHOR CONTRIBUTIONS

Conceptualization, H.L., and S.S.; Investigation, H.L., K. W., and Z. Y.; Writing—Original Draft, H.L., K.W., and Z.Y.; Writing—Review & Editing, H.L., K.W., Z.Y., and S.S.; Funding Acquisition, S.S.

DECLARATION OF INTERESTS

The authors declare no competing interests.

REFERENCES

Abbas, N., Li, Y., Ding, J.Z., Liu, J.P., Luo, H.B., Du, J., Xia, W.X., Yan, A., Wang, F., and Zhang, J. (2019). A facile synthesis of directly gas-phase ordered high anisotropic Sm–Co based non-segregated nanoalloys by cluster beam deposition method. Mater. Des. *181*, 108052.

Akdogan, O., Li, W., Hadjipanayis, G.C., and Sellmyer, D.J. (2011). Synthesis of single-crystal Sm-Co nanoparticles by cluster beam deposition. J. Nanopart. Res. *13*, 7005–7012.

Balasubramanian, B., Manchanda, P., Skomski, R., Mukherjee, P., Valloppilly, S.R., Das, B., Hadjipanayis, G.C., and Sellmyer, D.J. (2016). High-coercivity magnetism in nanostructures with strong easy-plane anisotropy. Appl. Phys. Lett. *108*, 1–5.

Barbir, F. (2013). PEM Fuel Cells : Theory and Practice (Academic Press).

Blanco, D.E., and Modestino, M.A. (2019). Organic electrosynthesis for sustainable chemical manufacturing. Trends Chem. *1*, 8–10.

Botte, G.G. (2014). Electrochemical manufacturing in the chemical industry. Electrochem. Soc. Interface *23*, 49–55.

Chadderdon, D.J., Xin, L., Qi, J., Qiu, Y., Krishna, P., More, K.L., and Li, W. (2014). Electrocatalytic oxidation of 5-hydroxymethylfurfural to 2,5-furandicarboxylic acid on supported Au and Pd bimetallic nanoparticles. Green. Chem. *16*, 3778.

Chen, Y., Vise, A., Klein, W.E., Cetinbas, F.C., Myers, D.J., Smith, W.A., Deutsch, T.G., and Neyerlin, K.C. (2020). A robust, scalable platform

for the electrochemical conversion of CO 2 to formate: identifying pathways to higher energy efficiencies. ACS Energy Lett. *2020*, 1825–1833.

Das, B., Balasubramanian, B., Manchanda, P., Mukherjee, P., Skomski, R., Hadjipanayis, G.C., and Sellmyer, D.J. (2016). Mn 5 Si 3 nanoparticles: synthesis and size-induced ferromagnetism. Nano Lett. *16*, 1132–1137.

Ding, S., Hülsey, M.J., Pérez-Ramírez, J., and Yan, N. (2019). Transforming energy with single-atom catalysts. Joule *3*, 2897–2929.

Dinh, C.T., Li, Y.C., and Sargent, E.H. (2019). Boosting the single-pass conversion for renewable chemical electrosynthesis. Joule *3*, 13–15.

Dong, Y.C., Jun, S.W., Yoon, G., Kim, H., Mun Yoo, J., Lee, K.S., Kim, T., Shin, H., Kumar Sinha, A., Gu Kwon, S., et al. (2017). Large-scale synthesis of carbon-shell-coated FeP nanoparticles for robust hydrogen evolution reaction electrocatalyst. J. Am. Chem. Soc. *139*, 6669–6674.

Fan, L., Xia, C., Zhu, P., Lu, Y., and Wang, H. (2020). Electrochemical CO2 reduction to high-concentration pure formic acid solutions in an all-solid-state reactor. Nat. Commun. *11*, 1–9.

Han, Z., Kortlever, R., Chen, H.Y., Peters, J.C., and Agapie, T. (2017). CO2 reduction selective for C≥2 products on polycrystalline copper with N-substituted pyridinium additives. ACS Cent. Sci. *3*, 853–859.

Hori, Y., Takahashi, I., Koga, O., and Hoshi, N. (2003). Electrochemical reduction of carbon dioxide at various series of copper single crystal electrodes. J. Mol. Catal. A Chem. *199*, 39–47.

Huang, X., Song, J., Hua, M., Xie, Z., Liu, S., Wu, T., Yang, G., and Han, B. (2020). Enhancing the electrocatalytic activity of CoO for the oxidation of 5-hydroxymethylfurfural by introducing oxygen vacancies. Green. Chem. *22*, 843.

Kevin, M., Van Geem, V.V.G., and Marin, G.B. (2019). Making chemicals with electricity. Science *364*, 734–735.

Kwon, Y., Jan Schouten, K.P., van der Waal, J.C., de Jong, E., and M Koper, M.T. (2016). Electrocatalytic conversion of furanic compounds. ACS Catal. *6*, 6704–6717.

LaGrow, A.P., Besong, T.M.D., AlYami, N.M., Katsiev, K., Anjum, D.H., Abdelkader, A., Costa, P.M.F.J., Burlakov, V.M., Goriely, A., and Bakr, O.M. (2017). Trapping shape-controlled nanoparticle nucleation and growth stages via continuous-flow chemistry. Chem. Commun. *53*, 2495–2498.

Lei, Q., Zhu, H., Song, K., Wei, N., Liu, L., Zhang, D., Yin, J., Dong, X., Yao, K., Wang, N., et al. (2020a). Investigating the origin of enhanced C 2+ selectivity in oxide-/hydroxide-derived copper electrodes during CO 2 electroreduction. J. Am. Chem. Soc. *142*, 53.

Lei, Y., Wang, Y., Liu, Y., Song, C., Li, Q., Wang, D., and Li, Y. (2020b). Designing atomic active centers for hydrogen evolution electrocatalysts. Angew. Chem. Int. Ed. *59*, 20794–20812.

Li, J., and Sun, S. (2019). Intermetallic nanoparticles: synthetic control and their enhanced electrocatalysis. Acc. Chem. Res. *52*, 2015–2025.

Li, K., and Sun, Y. (2018). Electrocatalytic upgrading of biomass-derived intermediate compounds to value-added products. Chemistry *24*, 18258–18270.

Li, Q., Wu, L., Wu, G., Su, D., Lv, H., Zhang, S., Zhu, W., Casimir, A., Zhu, H., Mendoza-Garcia, A., et al. (2015). New approach to fully ordered fct-FePt nanoparticles for much enhanced electrocatalysis in acid. Nano Lett. *15*, 2468–2473.

Loiudice, A., Lobaccaro, P., Kamali, E.A., Thao, T., Huang, B.H., Ager, J.W., and Buonsanti, R. (2016). Tailoring copper nanocrystals towards C2 products in electrochemical CO2 reduction. Angew. Chem. Int. Ed. *55*, 5789–5792.

Lu, B., Liu, Q., and Chen, S. (2020a). Electrocatalysis of single-atom sites: impacts of atomic coordination. ACS Catal. *10*, 7584–7618.

Lu, J., Guo, J., Song, S., Yu, G., Liu, H., Yang, X., and Lu, Z. (2020b). Preparation of Ag nanoparticles by spark ablation in gas as catalysts for electrocatalytic hydrogen production †. RSC Adv. *10*, 38583.

Ma, Y.Y., Wu, C.X., Feng, X.J., Tan, H.Q., Yan, L.K., Liu, Y., Kang, Z.H., Wang, E.B., and Li, Y.G. (2017). Highly efficient hydrogen evolution from seawater by a low-cost and stable CoMoP@C electrocatalyst superior to Pt/C. Energy Environ. Sci. *10*, 788–798.

Menezes, P.W., Panda, C., Garai, S., Walter, C., Guiet, A., and Driess, M. (2018). Structurally ordered intermetallic cobalt stannide nanocrystals for high-performance electrocatalytic overall water-splitting. Angew. Chem. Int. Ed. *57*, 15237–15242.

Millet, P., Ngameni, R., Grigoriev, S.A., Mbemba, N., Brisset, F., Ranjbari, A., and Etiévant, C. (2010). PEM water electrolyzers: from electrocatalysis to stack development. Int. J. Hydrogen Energy *35*, 5043–5052.

Muzzio, M., Li, J., Yin, Z., Delahunty, I.M., Xie, J., and Sun, S. (2019). Monodisperse nanoparticles for catalysis and nanomedicine. Nanoscale *11*, 18946.

Nam, D.H., De Luna, P., Rosas-Hernández, A., Thevenon, A., Li, F., Agapie, T., Peters, J.C., Shekhah, O., Eddaoudi, M., and Sargent, E.H. (2020). Molecular enhancement of heterogeneous CO2 reduction. Nat. Mater. *19*, 266–276.

Niu, G., Zhou, M., Yang, X., Park, J., Lu, N., Wang, J., Kim, M.J., Wang, L., and Xia, Y. (2016). Synthesis of Pt-Ni octahedra in continuous-flow droplet reactors for the scalable production of highly active catalysts toward oxygen reduction. Nano Lett. *16*, 3850–3857.

Orella, M.J., Román-Leshkov, Y., and Brushett, F.R. (2018). Emerging opportunities for electrochemical processing to enable sustainable chemical manufacturing. Curr. Opin. Chem. Eng. *20*, 159–167.

Ovalle, V.J., and Waegele, M.M. (2019). Understanding the impact of N-arylpyridinium ions on the selectivity of CO2 reduction at the Cu/electrolyte interface. J. Phys. Chem. C *123*.

Park, J., An, K., Hwang, Y., Park, J.E.G., Noh, H.J., Kim, J.Y., Park, J.H., Hwang, N.M., and Hyeon, T. (2004). Ultra-large-scale syntheses of monodisperse nanocrystals. Nat. Mater. *3*, 891–895.

Popović, S., Smiljanić, M., Jovanovič, P., Vavra, J., Buonsanti, R., and Hodnik, N. (2020). Stability and degradation mechanisms of copper-based catalysts for electrochemical CO2 reduction. Angew. Chem. Int. Ed. *31*, 2–13.

Vuyyuru, K.R., and Strasser, P. (2012). Oxidation of biomass derived 5-hydroxymethylfurfural using heterogeneous and electrochemical catalysis. Catal. Today *195*, 144–154.

Rønne, M.H., Cho, D., Madsen, M.R., Jakobsen, J.B., Eom, S., Escoudé, É., Hammershøj, H.C.D., Nielsen, D.U., Pedersen, S.U., Baik, M.H., et al. (2020). Ligand-controlled product selectivity in electrochemical carbon dioxide reduction using manganese bipyridine catalysts. J. Am. Chem. Soc. *142*, 4265–4275.

Santana, J.S., and Skrabalak, S.E. (2020). Continuous flow routes toward designer metal nanocatalysts. Adv. Energy Mater. *10*, 1–14.

Santana, J.S., Koczkur, K.M., and Skrabalak, S.E. (2017). Synthesis of Core@Shell nanostructures in a continuous flow droplet reactor: controlling structure through relative flow rates. Langmuir *33*, 6054–6061.

Schaidle, J.A., Habas, S.E., Baddour, F.G., Farberow, C.A., Ruddy, D.A., Hensley, J.E., Brutchey, R.L., Malmstadt, N., and Robota, H. (2017). Transitioning rationally designed catalytic materials to real "'working'" catalysts produced at commercial scale: nanoparticle materials. Catalysis *29*, 213–281.

Shen, Y., Zhou, Y., Wang, D., Wu, X., Li, J., and Xi, J. (2018). Nickel–Copper alloy encapsulated in graphitic carbon shells as electrocatalysts for hydrogen evolution reaction. Adv. Energy Mater. *8*, 1–7.

Siu, J.C., Fu, N., and Lin, S. (2020). Catalyzing electrosynthesis: a homogeneous electrocatalytic approach to reaction discovery HHS public access. Acc. Chem. Res. *53*, 547–560.

Sun, J., Wen, Z., Han, L., Chen, Z., Lang, X., and Jiang, Q. (2018). Nonprecious intermetallic Al 7 Cu 4 Ni nanocrystals seamlessly integrated in freestanding bimodal nanoporous copper for efficient hydrogen evolution catalysis. Adv. Funct. Mater. *1706127*, 1–7.

Tabrizi, N.S., Ullmann, M., Vons, V.A., Lafont, U., and Schmidt-Ott, A. (2009). Generation of nanoparticles by spark discharge. J. Nanopart. Res. *11*, 315–332.

Taitt, B.J., Nam, D.H., and Choi, K.S. (2019). A comparative study of nickel, cobalt, and iron oxyhydroxide anodes for the electrochemical oxidation of 5-hydroxymethylfurfural to 2,5-furandicarboxylic acid. ACS Catal. *9*, 660–670.

Thevenon, A., Rosas-Hernández, A., Peters, J.C., and Agapie, T. (2019). In-situ nanostructuring and stabilization of polycrystalline copper by an organic salt additive promotes electrocatalytic CO2 reduction to ethylene. Angew. Chem. Int. Ed. *58*, 16952–16958.

Wang, H., Tzeng, Y.K., Ji, Y., Li, Y., Li, J., Zheng, X., Yang, A., Liu, Y., Gong, Y., Cai, L., et al. (2020). Synergistic enhancement of electrocatalytic CO2 reduction to C2 oxygenates at nitrogen-doped nanodiamonds/Cu interface. Nat. Nanotechnol. *15*, 131–137.

Wang, J., Ding, H., Duan, G., Zhou, H., Song, C., Pan, J., and Li, C. (2019). Morphology-controllable gold hierarchically micro/nanostructured arrays prepared by electrodeposition on colloidal monolayer and their structurally related wettability. Chem. Phys. *523*, 63–69.

Wang, R., Dong, X.Y., Du, J., Zhao, J.Y., and Zang, S.Q. (2018a). MOF-derived bifunctional Cu3P nanoparticles coated by a N,P-codoped carbon shell for hydrogen evolution and oxygen reduction. Adv. Mater. *30*, 1–10.

Wang, Y., Han, P., Lv, X., Zhang, L., and Zheng, G. (2018b). Defect and interface engineering for aqueous electrocatalytic CO 2 reduction. Joule *2*, 2551–2582.

Wen, G., Ren, B., Park, M.G., Yang, J., Dou, H., Zhang, Z., Deng, Y.P., Bai, Z., Yang, L., Gostick, J., et al. (2020). Ternary Sn-Ti-O electrocatalyst boosts the stability and energy efficiency of CO2 reduction. Angew. Chem. Int. Ed. *59*, 12860–12867.

Xie, C., Niu, Z., Kim, D., Li, M., and Yang, P. (2020). Surface and interface control in nanoparticle catalysis. Chem. Rev. *120*, 1184–1249.

Xu, G., Zhao, J., Li, S., Zhang, X., Yong, Z., and Li, Q. (2011). Continuous electrodeposition for lightweight, highly conducting and strong carbon nanotube-copper composite fibers. Nanoscale *3*, 4215.

Yang, Y., Liang, X., Li, F., Li, S., Li, X., Ng, S.P., Wu, C.M.L., and Li, R. (2018). Encapsulating Co2P@C core–shell nanoparticles in a porous carbon sandwich as dual-doped electrocatalyst for hydrogen evolution. ChemSusChem *11*, 376–388.

Yin, Z., Yu, C., Zhao, Z., Guo, X., Shen, M., Li, N., Muzzio, M., Li, J., Liu, H., Lin, H., et al. (2019). Cu 3 N nanocubes for selective electrochemical reduction of CO 2 to ethylene. Nano Lett. *19*, 37.

You, B., Liu, X., Jiang, N., and Sun, Y. (2016). A general strategy for decoupled hydrogen production from water splitting by integrating oxidative biomass valorization. J. Am. Chem. Soc. *138*, 13639–13646.

Zhang, B., Zhang, J., Hua, M., Wan, Q., Su, Z., Tan, X., Liu, L., Zhang, F., Chen, G., Tan, D., et al. (2020a). Highly electrocatalytic ethylene production from CO 2 on nanodefective Cu nanosheets. J. Am. Chem. Soc. *142*, 13606–13613.

Zhang, L., Niu, G., Lu, N., Wang, J., Tong, L., Wang, L., Kim, M.J., and Xia, Y. (2014). Continuous and scalable production of well-controlled noble-metal nanocrystals in milliliter-sized droplet reactors. Nano Lett. *14*, 6626–6631.

Zhang, S., Fan, Q., Xia, R., and Meyer, T.J. (2020b). CO2 reduction: from homogeneous to heterogeneous electrocatalysis. Acc. Chem. Res. *53*, 255–264.

Zhao, X., Dr, P., Liu, D., Zhao, S.X., and Sajid, M. (2018). Production of 2,5-furandicarboxylic acid (FDCA) from 5-hydroxymethylfurfural (HMF): recent progress focusing on the chemical-catalytic routes. Green. Chem. 20, 5407–5552.

Zhou, J.H., Yuan, K., Zhou, L., Guo, Y., Luo, M.Y., Guo, X.Y., Meng, Q.Y., and Zhang, Y.W. (2019).

Boosting electrochemical reduction of CO2 at a low overpotential by amorphous Ag-Bi-S-O decorated Bi0 nanocrystals. Angew. Chem. Int. Ed. 58, 14197–14201.

Zhu, J., Hu, L., Zhao, P., Yoon, L., Lee, S., and Wong, K.Y. (2020). Recent advances in electrocatalytic hydrogen evolution using nanoparticles. Chem. Rev. 120, 851–918.

Zhu, W., Zhang, Y.J., Zhang, H., Lv, H., Li, Q., Michalsky, R., Peterson, A.A., and Sun, S. (2014). Active and selective conversion of CO2 to CO on ultrathin Au nanowires. J. Am. Chem. Soc. 136, 16132–16135.

Solar PV Cumulative Capacity.

Solar PV module prices.